Meteorologische Zeitschrift, Vol. **11**, No. 1, 5-12 (February 2002)
© by Gebrüder Borntraeger 2002

Article

Comparison of observed and simulated microwave land surface emissivities over bare soil

RALF BENNARTZ[1, *], KATJA PAAPE[2], JÜRGEN FISCHER[2] and TIM J. HEWISON[3]

[1] Freie Universität Berlin, Institut für Weltraumwissenschaften, Berlin, Germany
Current affiliation: University of Kansas, Department of Physics and Astronomy, Lawrence, Kansas, USA
[2] Freie Universität Berlin, Institut für Weltraumwissenschaften, Berlin, Germany
[3] Met Office, Y70 DERA, Farnborough, United Kingdom

(Manuscript received August 24, 2000; in revised form April 19, 2001; accepted June 11, 2001)

Abstract

In this paper we evaluate data obtained during the VALEM (Validation of Land Surface Emissivity Models) experiment, which took place in September 1998 near Ludwigslust in north-eastern Germany.

The emphasis of the field campaign was to generate datasets to validate land surface emissivity models in the microwave spectral range. We describe the approach to derive land surface emissivities from the observed data and compare observed and simulated land surface emissivities in order to further validate the Free University of Berlin's newly developed microwave emissivity model. This model explicitly accounts for any given type of structured surfaces by splitting the surface into large-scale facets and a small-scale surface roughness. A model description can be found in previous work (PAAPE et al., 2000) so that in the current paper we only present a brief overview on the model structure and concentrate on its validation at frequency ranges between 24 and 157 GHz.

The range of variability of the observed surface emissivity is about 18% (0.80–0.98) for the different frequencies and test sites. Comparing simulated and observed nadir emissivities we find deviations between 0.9% and 2.5% dependent on frequency. The deviations are in the range of uncertainty introduced by the various input parameters into the emissivity model. Comparing model results with radiometer observations at different incidence angles, we find that the model realistically resembles the variation of the surface emissivity with zenith angle at different frequencies.

Zusammenfassung

In diesem Artikel zeigen wir Ergebnisse der Validierung des Modells der Freien Universität Berlin zur Beschreibung des Emissionsvermögens von Landoberflächen im Mikrowellenbereich. Wir werten hierzu Daten aus, die während des VALEM-Experiments gemessen wurden. Dieses Experiment fand im September 1998 nahe Ludwigslust statt.

Das Bodenemissionsmodell erlaubt es, das Emissionsvermögen beliebig strukturierter Oberflächen zu simulieren, indem frequenzabhängig zwischen großskaligen und kleinskaligen Rauhigkeiten unterschieden wird. Eine Modellbeschreibung wurde bereits zuvor in PAAPE et al. (2000) veröffentlicht, so dass das Hauptaugenmerk im vorliegenden Artikel auf die Validierung des Modells im Frequenzbereich zwischen 24 und 157 GHz gelegt wird.

Der Schwankungsbereich des gemessenen Emissionsvermögens beträgt circa 18% (0,80–0,98) abhängig von Frequenz und Testgebiet. Der Vergleich des simulierten und gemessenen Emissionsvermögens von brachen Böden zeigt Abweichungen im Bereich zwischen 0,9% bis maximal 2,5% in Abhängigkeit von der Messfrequenz. Die gefundenen Abweichungen sind im Bereich der Ungenauigkeit, die durch die zahlreichen Eingangsdaten für das Modell zu erwarten ist. Sowohl die Frequenzabhängigkeit als auch die Abhängigkeit des Emissionsvermögens vom Beobachterzenitwinkel werden vom Modell gut wiedergegeben.

1 Introduction

In contrast to remote sensing techniques in the visible and infrared spectral range, the advantage in using microwave frequencies is that the atmosphere at most microwave frequencies is semi-transparent. Hence, even under cloudy conditions total column amounts of water vapour and other atmospheric constituents can be remotely sensed. Because of this semi-transparency, a large fraction of radiation emitted or scattered from the earth's surface is received at the observing radiometer. Remote sensing of atmospheric constituents in the microwave spectral range therefore requires exact knowledge of the emission characteristics of the underlying surface.

In the framework of the HYPAM-project the Free University of Berlin has developed a surface emissivity model that describes the emission characteristics of land surfaces (PAAPE et al., 2000; PAAPE, 2000). The

* Corresponding author: Ralf Bennartz, Department of Physics and Astronomy, University of Kansas, 1251 Wescoe Hall Dr., Lawrence, KS 66045, USA, e-mail: bennartz@ukans.edu

0941-2948/02/0011-0005 $ 03.60
DOI: 10.1127/0941-2948/2002/0011-0005
© Gebrüder Borntraeger, Berlin, Stuttgart 2002

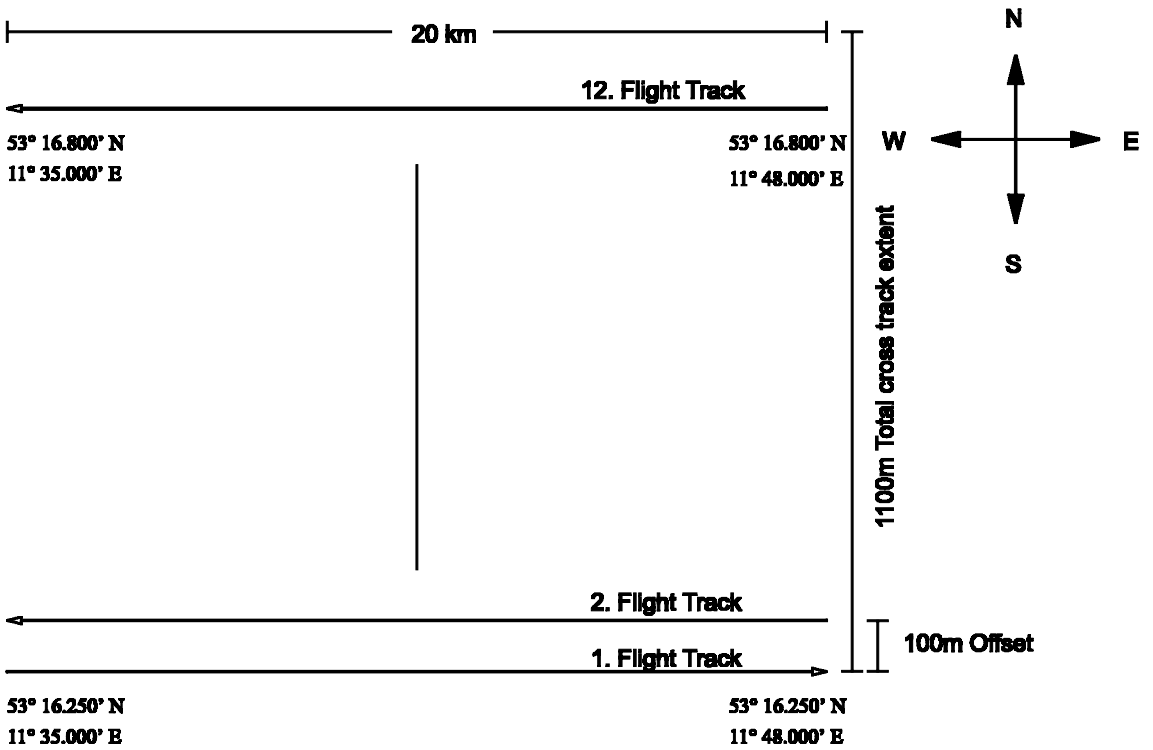

Figure 1: Flight pattern during the VALEM campaign.

aim was to develop a model that consistently describes the polarization state, the zenith angle dependency, and the frequency dependence of the emitted radiation in the relevant spectral range between 2.5 and 157 GHz. The physical principles for such models have been formulated (ULABY et al., 1986). The model developed by the authors and validated in this study is based on simple models of the dielectric behaviour of soils and is able to explicitly account for orographic and large scale surface effects. In previous investigations (PAAPE et al., 2000) we studied the model's response to artificial surfaces and did a validation study for the spectral range between 1 and 11 GHz using data of the RASAM-catalogue (WEGMÜLLER et al., 1994).

The current paper focuses on the validation of the model at higher frequencies between 24–157 GHz. As for the considered frequency range no existing datasets could be identified in the initial phase of the HYPAM-project, this validation required a comparably large experimental setup. Besides the radiometric observations, various atmospheric as well as surface and soil properties had to be measured in a dedicated field campaign (VALEM). During this experiment co-ordinated surface and airborne radiometer measurements for the frequency range between 24 GHz and 157 GHz were performed. In the following sections we will briefly describe the two-scale model which has been described in previous work (PAAPE et al., 2000). We will then discuss in detail the experimental setup of the VALEM campaign and describe the approach to derive land surface emissivities from the aircraft observations. In Section 5 we will compare simulated and observed emissivities and discuss the results with emphasis on the zenith angle and the frequency dependence of the model.

2 The two-scale model

The two-scale model developed at the Free University of Berlin has been described in PAAPE et al. (2000) and in more detail in PAAPE (2000), so that we only give a short description of those components critical for the subsequent considerations. For more detailed information we refer to the above publications. The main difference between our model and other published models is its ability to explicitly account for any type of structured surface. The advantage of such approach is that arbitrary surfaces may be simulated and that besides the zenith angle dependence also the azimuthal dependence of the emitted radiation field can be modelled. Especially for oriented surfaces like row structures or tilted surfaces conventional models are not able to resolve their azimuthal dependence.

The model separates two types of roughness heights. Firstly large-scale roughness, which can be treated in the geometric optics approximation and secondly small-scale roughness, which determines the emittance behaviour of the considered surface. This approach is not new and has been used for the determination of sea surface emissivity for several years (e.g. SCHRADER, 1995). However, other models typically use parameterizations of the distribution of the large scale roughness elements (facets), so that the azimuthal distribution of the observed brightness temperature field may not be resolved.

Table 1: Observed surface characteristics of the four test sites.

Site	*Temperature* [°C]		*Moisture* [%]		*LAI*		*rms-height* [cm]		
Index	*Average*	*Std. dev.*	*Average*	*Std. dev.*	*Average*	*Std. dev.*	*All reliefs*	*Average*	*Std. dev.*
1	22.7	2.6	15.5	4.2	–	–	1.1 1.3 1.2 1.3	1.2	0.1
2	19.0	1.1	16.0	2.9	–	–	1.5 0.7 0.7	1.0	0.6
3	19.0	0.7	20.5	2.9	–	–	0.6 0.6	0.6	0.1
4	–	–	–	–	3.0	0.8	–	–	–

3 The validation of land surface emissivity models (VALEM) campaign

The VALEM campaign was performed in co-operation between the Free University of Berlin and the Meteorological Research Flight department of the Met Office of the UK. It was set up to provide a dataset to validate land surface emissivity models designed to work in the range of current spaceborne passive microwave radiometers. Besides the aircraft observations, several surface parameters had to be measured. All measurements were taken on September 20, 1998. At that day the weather over northern Germany was governed by a high pressure system with center over Denmark. The flights were performed between 12:50 MESZ and 14:15 MESZ. Relative humidity at the surface was about 70%, average air temperatures about 17°C. Moderate convection resulted in about $\frac{6}{8}$ cumulus with cloud base at around 500 m. In addition about $\frac{3}{8}$ cirrus were found at higher altitudes. The VALEM dataset consists of surface and airborne observations described below.

3.1 The test sites

We choose four different agricultural areas as test sites. Each test site covered an area between 1 km × 1 km and 2 km × 2 km, so that despite the large footprint size of the airborne radiometers sufficient aircraft observations were available. In order to maximise the amount of usable data a flight pattern according to Fig. 1 was chosen. All four test sites were aligned in east- west direction, so that each flight track depicted in Fig. 1 overpassed all four areas. The different flight tracks were about 100 m apart, so that between 20 and 70 independent observations were collected for each site.

3.2 Surface observations

Surface measurements include all relevant parameters, necessary to describe the state of the surface and its emission characteristics. Surface temperature, surface roughness, soil moisture, and soil texture were measured.

Surface temperature was observed using the aircraft's Heimann infrared radiometer, which measures the radiometric skin temperature in the 8–14 μm range. This ensures coincident microwave and infrared measurements, which is especially important given the temporal variability of the surface temperature. The physical temperature of the surface was derived using published algorithms (VALOR and CASELLES, 1996).

Surface roughness was determined using a laser-reliefmeter (HELMING, 1992; WEIMANN, 1996). This instrument measures two-dimensional profiles of surface height over an 1 × 1 m^2 area with a horizontal resolution of 0.3 mm and a vertical resolution of 0.3 mm using laser-triangulation. The laser-reliefmeter observations are extremely time consuming, as the entire area is scanned at very high resolution. The typical time for one complete relief was about 70 minutes. Therefore only 2–4 sample areas could be measured on each test site, which were taken within 6 hours of the flight time.

Soil moisture was measured using a time-domain-reflectometer (TDR-sonde, kindly provided by Dr. M. SCHOENERMARK, DLR-Adlershof). The penetration depth of microwave radiation for soils is about 0.06 λ–0.2 λ according to WILHEIT (1978) and WANG (1987). Hence, the relevant soil moisture for the microwave emissivity is in the top 2 mm of the soil. Although the TDR-method does not allow to derive soil moisture in millimeter-thick layers, we accounted for this by trying to probe the moisture of the uppermost six centimeters, which is the best achievable result using TDR-sondes. Also, since there might be a strong diurnal cycle in soil moisture in the uppermost part of the soil, we performed the soil moisture observations timed exactly according to the C-130 overpasses.

The **soil texture** of the different sites was determined to be 40% sand, 20% silt and 40% clay, according to the

Table 2: Sensor characteristics of the MARSS and Deimos according to HEWISON (2001).

	Deimos		*MARSS*	
Frequency	23.8	50.1	89.0	157.0
Integration time	50 ms		80 ms	
Scan period	3 s		3 s	
Beamwidth (3dB)	11°		10°	
Nadir looks	+35° to −5°		+40° to −40°	
Zenith looks	–		+40° to −40°	
Polarisation	H, V		mixed	H or V
Sensitivity	±0.6 K	±0.6 K	±0.3 K	±0.5 K
Absolute accuracy	±1.5 K	±1.5 K	±0.9 K	±0.8 K

geological maps of Mecklenburg-Vorpommern (SCHEFFER and SCHACHTSCHABEL, 1989). Test site 4 was the only vegetated site, covered by corn in its final growing stage. As we focus on the validation of the emissivity model for bare soils, site 4 was excluded from this study.

The surface characteristics of the four test sites are listed in Tab. 1. Test sites 1 to 3 were essentially vegetation-free, and their rms-height varied between 0.6 cm and 1.2 cm. Volumetric soil moisture for all four fields was in the range between 15 and 20%, with a standard deviation of 3–4%.

3.3 Airborne observations

Airborne observations were performed by the Met Office's Hercules C-130. Two microwave radiometers were available onboard the C-130, namely the Microwave Airborne Radiometer Scanning System (MARSS) and the Deimos. Tab. 2 lists the relevant characteristics of both instruments. More detailed information about both systems can be found in HEWISON and ENGLISH (1999). In addition to microwave observations, a number of auxiliary data was sampled by the C-130, including time, GPS navigation, surface temperature, dew point, air pressure and temperature at flight level.

To obtain the highest possible resolution of the passive microwave observations, all flights were performed at the lowest allowed altitude of 500 ft. According to the beamwidth, integration time (see Tab. 2), and the aircraft velocity of approximately 100 m/s the footprint size of the MARS and Deimos observations at altitudes of 500 ft is roughly 30 m and samples are taken every 300 m along track.

Tab. 3 shows the observed mean values and standard deviations of the aircraft observations exemplarily for test site 3 and nadir respective zenith observations. A monotonic increase with frequency can be seen for the upwelling radiances. The variability of the observations is highest for the upwelling low frequency observations and the downwelling low frequency observations. The infrared estimate of surface temperature and the estimate of the average air temperature between surface and aircraft are stable within 1.1 K respective 0.5 K. While the absolute values of the parameters vary slightly from test site to test site, the variability of the parameters for any given test site shows very similar results.

Table 3: Average values and standard deviations for the aircraft measurements for test site 3. The total number of observations for test site 3 was N=26. The zenith radiances $T_B^{\downarrow}$ marked with an asterisk have been calculated from other observations (see text for details).

	24 GHz	50 GHz	89 GHz	157 GHz
$T_B^{\uparrow}$ [K]	278.0±6.6	282.0±1.9	282.4±1.6	290.3±0.7
$T_B^{\downarrow}$ [K]	34.8±1.7*	87.5±1.5*	62.5±4.0	160.9±5.3
T_S [K]	293.7±1.1			
T_A [K]	290.5±0.5			

4 Derivation of surface emissivity from aircraft observations

Fig. 2 depicts the observation geometry of the airborne spectrometers and the relevant contributions of different parts of a non-scattering atmosphere and the surface to the total observed signal. The signal received at the aircraft can be written as:

$$T_B^{\uparrow}(\theta) = \underbrace{\underbrace{[T_B^{\downarrow}(\theta)\,\tau(\theta) + T_A\,(1-\tau(\theta))]}_{(a)}\,(1-e(\theta))\,\tau(\theta)}_{(b)} + \underbrace{T_S\,e(\theta)\,\tau(\theta)}_{(c)} + \underbrace{T_A\,(1-\tau(\theta))}_{(d)} \tag{4.1}$$

where z is the aircraft altitude, θ the zenith angle of the observation, $T_B^{\uparrow}$ and $T_B^{\downarrow}$ the upwelling respective downwelling brightness temperature at aircraft altitude, $e(\theta)$ the surface emissivity, T_S the surface temperature, and τ and T_A the transmission and average temperature of the layer between the surface and aircraft. Term (a) in Equation 4.1 represents the downwelling brightness

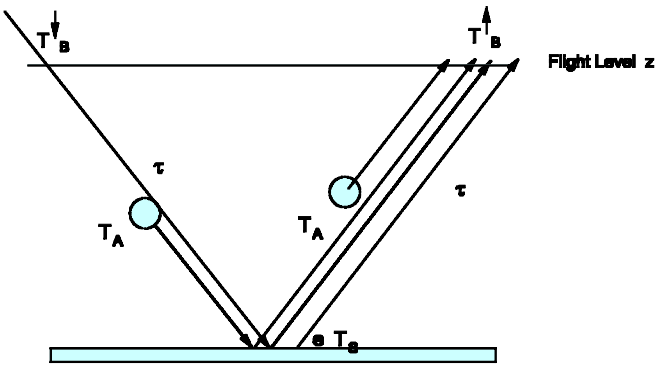

Figure 2: Observation geometry for the aircraft observations and different contributions to the total signal received at the aircraft (see Equation 4.1).

temperature $T_{B,S}^{\downarrow}$ at the surface. Term (b) is the reflected and transmitted part of the downwelling radiation as received at aircraft altitude. Term (c) is the radiation emitted from the surface received at the aircraft and (d) the upwelling radiation emitted from the atmosphere below the aircraft. In our case term (c) is the predominant term in Equation 4.1 since τ is close to one because of the low aircraft altitude and ε is in the range of 0.8–1.0. Uncertainties in the estimation of the surface temperature therefore contribute most strongly to the estimation of surface emissivity.

Equation 4.1 can formally be solved for the surface emissivity:

$$e = \frac{T_B^{\uparrow}/\tau - (T_A(1-\tau)/\tau) - \tau T_B^{\downarrow} - T_A(1-\tau)}{T_S - \tau T_B^{\uparrow} - T_A(1-\tau)} \qquad (4.2)$$

Besides the upwelling brightness temperature $T_B^{\uparrow}$ a set of other parameters has to be observed to obtain the surface emissivity. In the following we give brief description on how the components of Equation 4.2 were derived from the measurements.

4.1 Estimation of the average temperature T_A and transmission τ between surface and aircraft altitude

The temperature of the layer between aircraft altitude (500 ft) and surface has been averaged from the surface temperature and the temperature measured at aircraft altitude. The transmission has been derived by first using the surface and aircraft estimates of relative humidity and temperature to derive the column amount of water vapour between surface and aircraft altitude. The transmission at the four frequencies under consideration was then derived according to LIEBE (1985). While LIEBE (1985) is not the most recent parameterization of atmospheric transmission, results are only slightly affected by variations in the transmission of the atmosphere between surface and aircraft (see discussion in Section 5.3).

4.2 Estimation of surface temperature T_S

Surface temperature has been estimated from the Heimann radiometer onboard the C-130. To obtain surface temperature from the spectrometer, an atmospheric correction has to be performed. The dominant absorber in the infrared region between 8–14 μm is water vapour. The atmospheric correction follows the method described in HEWISON and ENGLISH (1999). An estimate for the accuracy can be obtained from comparing the aircraft observations with the measurements at surface. The maximum deviation between both was found to be 1.4 K and is about 50% of the standard deviation associated with either the aircraft or surface observations.

4.3 Estimation of zenith radiances $T_B^{\downarrow}$ at 24 and 50 GHz

MARSS directly observes zenith radiances at 89 and 157 GHz. For the two channels of Deimos at 24 and 50 GHz no direct observation of the downwelling radiation field were available. The zenith radiances of the Deimos thus were estimated from the known zenith radiances of the MARSS and radiative transfer calculations. The radiative transfer simulations were based on the parameterization of water vapour and cloud liquid water absorption according to LIEBE (1985). We used a simple emission model to calculate the downwelling radiance field at aircraft altitude for all four frequencies of MARSS and Deimos for a set of radiosonde profiles including artificial non-precipitating clouds with liquid water path below 0.3 kg/m^2. On the resulting dataset we performed a regression to estimate the low frequency zenith radiances from the high frequency radiances. The maximum rms-error of the regression is 2.5 K at 50 GHz and 2.3 K at 23 GHz. These regressions were used to estimate the downwelling radiance field at 24 and 50 GHz from the observed ones at 89 and 157 GHz.

5 Comparison of observed and simulated emissivities

Using Equation 4.2 we could now calculate the surface emissivity from the aircraft observations. At the same time surface emissivity was calculated from the surface observations using the two-scale model. In the following we compare the results of both for nadir emissivity and for the off-nadir observations at 35° to 40°.

5.1 Nadir emissivity

Fig. 3 shows the comparison of observed and simulated surface emissivities for the nadir observations. Direct co-location between the aircraft and the surface data did not seem reasonable since the footprint size of the aircraft observations and the surface data differ too much. Therefore we averaged over all available observations for a given test site and compared the average values. The error bars depict the standard deviation obtained for

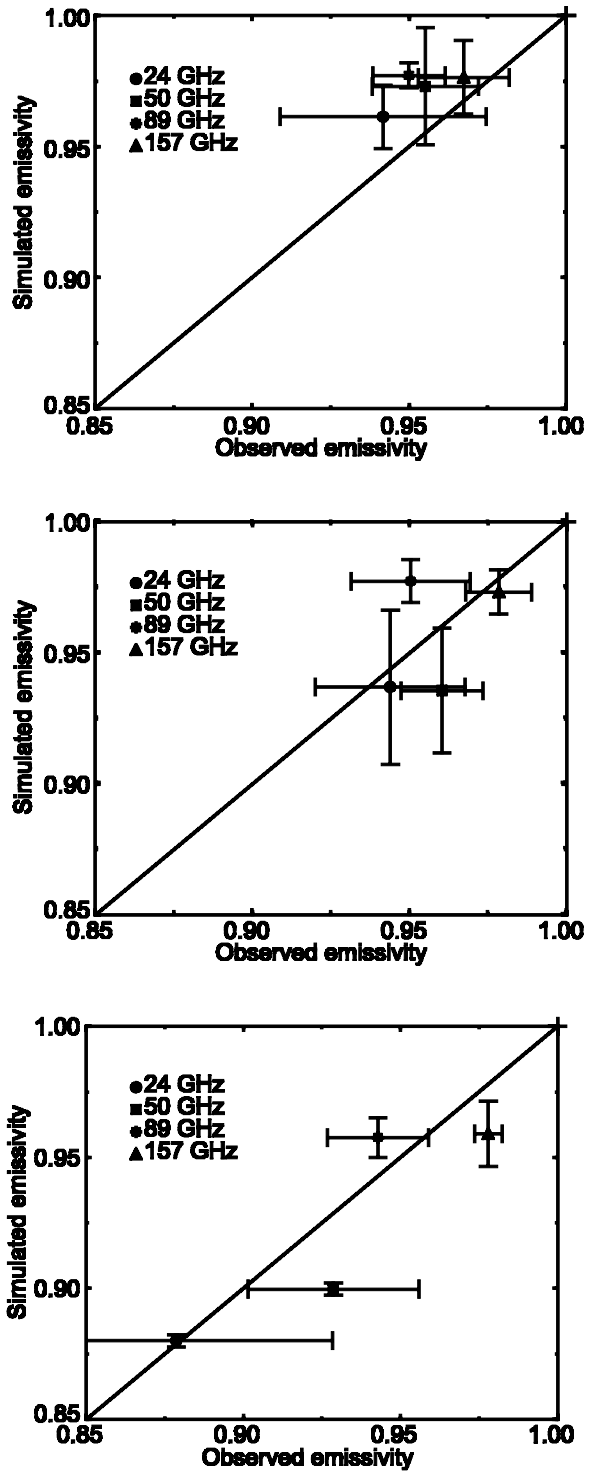

Figure 3: Comparison of observed and simulated surface emissivities for the test sites 1 (upper panel), 2 (mid panel), and 3 (lower panel) for nadir view. Error bars represent one standard deviation.

the different observations for each test site. For test site 1 both, the simulated and the observed emissivity vary only within a very narrow range and the standard deviation at a given frequency exceeds the variability between the different frequencies. These small variations arise from the surface characteristics of test site 1. As shown in Tab. 1, test site 1 exhibits the lowest soil moisture and the highest soil roughness of all test sites. Test site 2 shows less roughness but roughly the same soil moisture (see Tab. 1). Correspondingly the variability of the surface emissivities is somewhat higher. Test site 3 is even smoother and exhibits a significantly higher amount of soil moisture than the other two test sites. This results in a significant variability of surface emissivity with frequency. Minimum values around 0.87 are found for the very low frequencies (24 GHz) and maximum values around 0.96 for the higher frequencies.

For the very high frequencies the entire variability of surface emissivity within all test sites is comparably small. This is caused by an overlap of two effects. Firstly, the sensitivity to soil moisture decreases with frequency. Secondly, at high frequencies (small wavelength) even small absolute surface roughnesses appear radiometrically rough. Therefore, the variations in surface roughness as well as soil moisture have the strongest influence on the low frequency channels. These physical relations are found in the observed data and are realistically resembled by the model.

5.2 Off-nadir emissivity

Fig. 4 shows the simulated and observed emissivity for the Deimos and MARSS off-nadir observations for the horizontal and vertical polarization. The polarization of MARSS' 89 GHz channel is not aligned in this way, and has thus been excluded from the comparison. The deviations between simulated and observed emissivities range between minimum 0.2% for test site 1 and maximum 4.6% for test site 3. All three test sites show an increase of surface emissivity with frequency, both in the simulated and the observed data. Especially for test site 1 the different relief observations reveal a broad variety of different simulated emissivities. This can be seen from the large error bars of $\pm$ 0.05. Similar to the nadir observations the comparably smooth test site 3 shows little variations in simulated emissivity, but still considerable variability in the observed ones. This may result from variations of soil moisture or roughness that have not been represented by the in-situ observations.

5.3 Error analysis

Tab. 4 shows the sensitivity of Equation 4.2 to the various input parameters. A value of one in this table would

Table 4: Sensitivity of surface emissivity to the various input parameters in Equation 4.2.

		24 GHz	50 GHz	89 GHz	157 GHz
$T_B^{\uparrow}$	$[\%/K]$	+0.40	+0.51	+0.99	+0.45
$T_B^{\downarrow}$	$[\%/K]$	-0.01	-0.03	-0.02	-0.02
T_S	$[\%/K]$	-0.35	-0.47	-0.82	-0.42
T_A	$[\%/K]$	-0.01	-0.02	-0.13	-0.01
τ	$[\%/\%]$	-0.10	-0.10	-0.03	-0.02

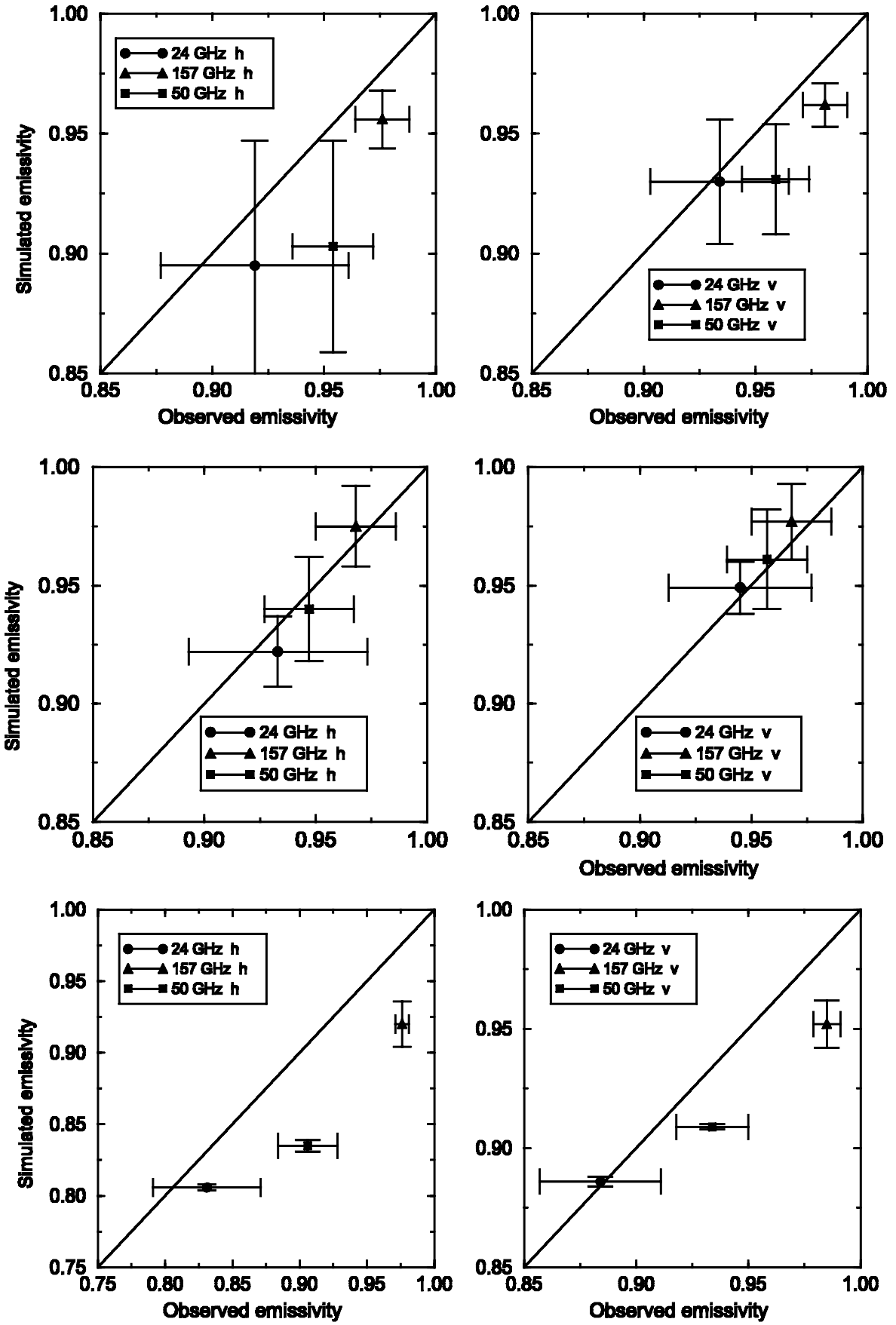

Figure 4: Off-nadir observations. Sites as in Fig. 3. Left column: horizontal polarization, right column: vertical polarization.

correspond to an increase in surface emissivity by 0.01 if the according input parameter is changed by 1 K (or 1% for the transmission τ). Not surprisingly, the most sensitive parameters are the observed brightness temperature at nadir and the surface temperature. The ratio between these two variables almost entirely defines the surface emissivity for the test sites under investigation. All other parameters contribute only to a small amount to the emissivity estimate. This is because the layer between the aircraft and the surface is only about 200 m thick, so that its transmission is high. The reflected part of the downwelling radiation does also not contribute much, since the emissivity in general is high and therefore only a small amount of the downwelling radiation is reflected back toward the sensor.

Comparing these results to the standard deviations of the measurements as given in Tab. 3, the largest part of the observed variability of the retrieved surface emissivity at low frequencies is due to variations in the observed upwelling microwave radiation. While the surface temperature estimate is stable within 1.1 K, especially the 24 GHz measurements show considerable variations (6.6 K). At the higher frequencies, both the surface temperature estimates and the upwelling microwave radiation contribute equally to the uncertainty.

6 Conclusions

The VALEM dataset provides a set of observations that allow the validation of microwave land surface emissivity models in the spectral range between 24 and 157 GHz. Since surface emissivity can not be observed directly, the validation has to rely on observation of other parameters from which the actual surface emissivity can be estimated. For the particular case discussed here several complications hamper the comparison of the simulated and observed emissivities. First of all, despite the low aircraft altitude the footprint size of the airborne radiometers does not coincide with the relief observation. Other necessary parameters could not be observed directly and had to be determined via radiative transfer calculations. In view of these difficulties we find a surprisingly good agreement between observed and simulated emissivities with maximum deviations of 2.5% for nadir observations and 4.6% for off-nadir observations. The frequency dependence of the emissivities is also well resembled by the model. In conjunction with the low frequency validation results published in PAAPE et al. (2000), the results presented here indicate the model's validity over the frequency range from 1–157 GHz.

Acknowledgments

The authors would like to thank Dave KINDRED and his colleagues at the Met Office of the UK for their excellent work in running the VALEM campaign. This work was supported by the DFG under contract number Fi 435/6-1 and by the EU program STAAARTE (Scientific Training and Access to Aircraft for Atmospheric Research Throughout Europe).

References

HELMING, K., 1992: Die Bedeutung des Mikroreliefs für die Regentropfenerosion. – Dissertation, Fachbereich Landschaftsentwicklung, Technische Universität Berlin, 127 pp.

HEWISON, T.J., 2001: Airborne measurements of forest and agricultural land surface emissivity at millimetre wavelengths. – IEEE Trans. Geosci. Remote Sensing **39**, 393–400.

HEWISON, T.J., S.J. ENGLISH, 1999: Airborne retrievals of snow and ice surface emissivity at millimetre wavelengths. – IEEE Trans. Geosci. Remote Sensing **37**, 1871–1879.

LIEBE, H.J., 1998: An updated model for millimeter wave propagation in moist air. – Radio Sci. **20**, 1069–1089.

PAAPE, K., 2000: Simulation der Emissionseigenschaften von Landoberflächen im Mikrowellenbereich mittels eines Zweiskalenmodells. – Dissertation, Institut für Weltraumwissenschaften, Freie Universität Berlin, 103 pp. ISBN 3-931545-16-4.

PAAPE, K., R. BENNARTZ, J. FISCHER, 2000: A combined two-scale model for microwave emissivities of land surfaces. – In: Microwave radiometry and remote sensing of the earth's surface and atmosphere, PAMPALONI, P., S. PALOSCIA (Eds.), VSP Zeist, The Netherlands, 317–344. ISBN 90-6764-318-1.

SCHEFFER, F., P. SCHACHTSCHABEL, 1989: Lehrbuch der Bodenkunde, 12. Auflage. – F. Enke Verlag, Stuttgart, 494 pp.

SCHRADER, M., 1995: Ein Dreiskalenmodell zur Berechnung der Reflektivität der Ozeanoberfläche im Mikrowellenfrequenzbereich. – Dissertation, Institut für Meereskunde, Christian-Albrechts-Universität, Kiel, 97 pp.

ULABY, F.T., R.K. MOORE, A.K. FUNG, 1986: Microwave Remote Sensing, Active and Passive, Volume III: From Theory to Applications. – Artech House, Dedham, MA, USA, 1100 pp.

VALOR, E., V. CASELLES, 1996: Mapping of land surface emissivity from NDVI: Application to European, African, and South American areas. – Rem. Sens. Environm. **57**, 167–184.

WANG, J., 1987: Microwave emission from smooth bare fields and soil moisture sampling depth. – IEEE Trans. Geosci. Remote Sensing **GE-25**, 616–622.

WEGMÜLLER, U., C. MÄTZLER, R. HÜPPI, E. SCHANDA, 1994: Active and passive microwave signature catalogue on bare soil. – IEEE Trans. Geosci. Remote Sensing **3**, 698–702.

WEIMANN, A., 1996: Bestimmung der Bodenfeuchte mittels aktiver Mikrowellensensoren. – DLR Forschungsbericht **96-38**.

WILHEIT, T.T., 1978: Radiative transfer in a plane stratified dielectric. – IEEE Trans. Geosci. Electron. **GE-16**, 138–143.